CRITICAL SALINITY FOR ARCHIE – NON ARCHIE MODELS IN THE JAUF SANDSTONE RESERVOIR, SAUDI ARABIA

Salih Saner and Mimoune Kissami

The Research Institute, King Fahd University of Petroleum and Minerals,
Dhahran 31261, Saudi Arabia

ABSTRACT

In this case study, the effect of clay content on the resistivity of the Jauf Sandstone was investigated through multiple-salinity electrical tests on nine 1.5 inch diameter and 2.5 inch long core plug samples. Tested samples were selected from a semi-consolidated, brownish, porous and permeable quartz arenite facies from three different wells. Samples contain dominantly authigenic illite and minor chlorite clays lining the pores. Experiments were conducted under 65 °C temperature and 2,000 psi confining pressure condition. Ten different brine concentrations, starting with the highest concentration (250 kppm), were circulated sequentially through the samples while recording the electrical conductivity changes of the rock.

Tests showed a 4 to 8 percent clay effect (BQv / Cw) on the electrical conductivity. The low clay effect is due to: (1) low clay percentage, (2) illite and chlorite type clays, which have a low-to-moderate cation exchange capacity, and (3) high formation brine concentration in the reservoir. The low resistivity in the reservoir is not due to clay conductance, but it is due to microporosity that is caused by the pore-lining or filling clay texture. The critical salinity corresponding to the commonly accepted 10 percent clay effect cutoff is calculated to be 100 kppm. Although the Archie model is valid for water saturation interpretation in the reservoir, low salinity brine effects, such as mud filtrate or injection water, requires the consideration of appropriate shaly sand models.

INTRODUCTION

The Jauf Sandstone is a gas and gas condensate reservoir in the southern part of the Ghawar structure in the eastern province of Saudi Arabia. Reservoir rock contains clay minerals which affect petrophysical and reservoir properties. When clay is present in the reservoir rock, the Archie [1] relationship can become invalid depending on the occurrence of clay and the salinity of the formation brine. The shaly-sand problem basically is the correction of the resistivity logs for conductive clay mineral effects. Without this correction, the calculated water saturation is higher than the true water saturation.

Electrochemical theory suggests that the surfaces of clay minerals carry excess negative charges as a result of the substitution of certain positive ions by others of lower valence. When the clays are brought in contact with an electrolyte, these negative charges on the clay surface attract positive ions and repulse the negative ions present in the solution. As a

result, an electrical ionic double layer is generated on the exterior surfaces of the clays. The accumulation of ions near the charged surface makes a contribution to the total solution conductivity. Therefore, not only does the quantity and type of clay affect the excess conductivity caused by the electric double layers, but also its distribution and morphology [2,3].

The Waxman and Smits model [4] has been used to interpret the conductivity of a wide range of shaly rock samples. This model is based on the experimental results of a wide variety of core samples. The generalized Waxman - Smits equation for water saturated shaly sands is as follows:

$$C_o = 1/F^* (BQ_v + C_w) \quad (1)$$

where:

- C_o: Conductivity of rock fully saturated with brine solution (mho/m)
- F^*: Formation factor for shaly sandstone
- Q_v: Cation exchange capacity per unit pore volume (meq/cc)
- C_w: Conductivity of the brine (mho/m)
- B: Equivalent conductance of clay exchange cations at room temperature (mho cm^2/meq)

In clay-bearing rocks, if the conductivity of clay is smaller than the conductivity of brine, the Waxman-Smits assumption of a constant F^* is valid. However, where the conductivity of clay exceeds the conductivity of brine, F^* may no longer be constant, implying that the Waxman-Smits assumption of a constant F^* is not always valid [5].

In this study the mineral and pore characteristics of the Jauf reservoir samples were determined with an emphasis on clay minerals, and multiple salinity tests were conducted on nine preserved core plugs. Tests were performed using ten brines of different concentrations and a C_o versus C_w relation for each tested sample was developed.

GEOLOGICAL SETTING

The Jauf Formation is a 463 foot thick sandstone-shale sequence of the Devonian age that overlies the Tawil Formation and is overlain by the Jubah Formation. Due to the shale domination in the upper part of the Jauf Formation, the reservoir zone starts 94 feet below the formation top (Figure 1). Dominant sandstone in the lower part decreases upward while shale increases. The reservoir sequence is subdivided into three lithofacies intervals based on the proportions of shale and sandstone:

1. Black shale interval (206 feet)
2. Heterolithic greenish gray sandstone interval (111 feet)
3. Yellowish quartzitic interval (56 feet)

The lowermost yellowish quartzitic interval is almost shale-free, but is very tight due to an extensive quartz overgrowth that gives the rock an orthoquartzitic character. The sandstone inter-layers within the upper two lithofacies are mostly poorly porous and have low permeability. However, some 5-15 foot thick, highly porous and permeable, semi-consolidated gas bearing inter-layers are present in the sequence. Brownish core plug samples from these sand bodies look oil stained, but iron bearing clay is the cause of the brownish color. Fining upward patterns with a cross-stratified lower part and a horizontal laminated upper part implies distributary channel type deposition for these intervals. Water-free gas flow appeared in well tests in spite of low resistivity log readings (around 1 and 2 ohm-m) in these zones.

MINERAL AND PORE CHARACTERISTICS

The mineralogy, texture, pore characteristics, and clay content of the reservoir rock samples were analyzed via thin section and Scanning Electron Microscopy (SEM) techniques. Composition and mineralogy were elaborated by the Energy Dispersive Spectrometer (EDS) attached to the SEM, and X-ray Diffraction (XRD) analyses.

Mineralogy and Texture

Almost all samples consist of quartz, some feldspar (microcline), minor heavy minerals, and clay minerals. Quartz forms about 90 to 95 percent of the rock, while K-feldspar grains are about 2 to 4 percent. Large quartz grains are rounded terrigenic sand particles whereas small grains are idiomorphic authigenic crystals (Figure 2A and 2B). Most of the feldspars are altered to form authigenic clay, which is about 2 to 5 percent, and mostly occurs as pore lining or pore filling forms. Quartz overgrowths and poikilotopic calcite (3 to 5 mm patches) are other pore filling materials.

Grains are 100-500 micron size and medium-to-poorly sorted. Sieve analysis revealed a fine-to-medium sandstone [6] with the presence of very few coarse grains (> 500 microns) and a 9.85 percent silt+clay fraction. The mean grain size of 212 microns corresponds to fine sand. The bimodal distribution indicates two origins for the particles, where fine angular grains are authigenic quartz crystals and coarse rounded grains are terrigenic sand particles.

Clay Minerals

XRD and XRF analyses show over 90 percent quartz in the samples. Illite and clinochlore (chlorite) are commonly occurring clay minerals. Montmorillonite and saponite occur in minor amounts in a few samples. K-feldspar, ferroan and sylvite are the other two common minerals, but sylvite was probably precipitated from pore brine during drying of the samples.

Various clay morphologies and associated micro pore types are observed in the SEM views. The samples demonstrate authigenic illite in the pore filling, lining, and bridging forms. Commonly, a mat type illite covers the quartz grains, then it grows as ribbons with bifurcated edges, and towards the center of the pore spaces it becomes filamentous

(Figures 3A and 3B). Chlorite also occurs in pore lining form. A close-up SEM photo in Figure 3C shows a pore-lining authigenic chlorite consisting of 10-micron pseudo hexagonal crystals perpendicular to the sand grain surface and some minor filamentous illite, which in turn forms bridges between some chlorite crystals. Figure 3D shows a honeycomb type mixed layer illite/smectite occurrence, which is rare in the Jauf reservoir.

Porosity Characteristics

Interparticle macroporosity is visible in highly porous samples, in spite of clay, silica, and calcite type secondary precipitations in the pore spaces. Visible macroporosity in thin section photomicrographs is about 10 to 20 percent and pore size ranges from 50 to 200 microns (Figure 2). Interparticle pores in fine-grained silty samples are mostly filled with clay, and porosity therefore is low and in micro form in fine grained samples. Porosity remaining as micropores between the clay particles are highlighted by Rhodamine-B dyed epoxy intrusion in thin section photomicrographs. The micropore forms associated with clay are seen in Figure 3. Laminated samples comprise alternating relatively coarse-grained macroporosity and fine-grained microporosity laminae in millimeter scale.

BASIC PROPERTIES OF TESTED SAMPLES

The multi-salinity electrical tests were conducted on nine preserved core plug samples to determine the clay effect on the resistivity of the Jauf Sandstone. Samples 1/1, 1/2, 1/3, and 4 were homogeneous brown quartz arenites. Sample 1/7 was also homogeneous sandstone, which was differentiated by its milky white color. Sample 1 was a brown sandstone characterized by many 3 mm white spots of poikilotopic calcite cemented patches, whereas Samples 393, 395, and 1/6 were laminated heterogeneous sandstones. The basic core properties of the samples tested are shown in Table 1. All the samples contain authigenic clay lining or filling the pore spaces. Porosities of the tested samples were between 14.08 and 24.79 percent and their permeabilities were between 3.15 and 711.43 mD.

Table 1. Basic core properties of samples used in multi-salinity tests.

Sample No.	Length (cm)	Diameter (cm)	Bulk Volume (cc)	Dry Weight (g)	Grain Density (g/cc)	Pore Volume (cc).	Porosity (%)	Perm (mD)
393	7.560	3.698	81.198	157.568	2.523	18.720	23.10	839.3
395	7.546	3.773	84.368	168.403	2.511	19.860	20.50	19.2
1/1	6.886	3.775	77.071	154.645	2.668	19.105	24.79	196.300
1/2	7.116	3.783	79.983	170.527	2.681	16.368	20.46	63.639
1/3	7.189	3.772	80.334	164.396	2.665	18.644	23.21	711.429
1/6	7.120	3.785	80.113	181.131	2.670	12.279	15.33	3.150
1/7	7.138	3.791	80.570	179.143	2.588	11.338	14.08	15.610
1	5.891	3.710	68.683	127.914	2.543	14.423	21.00	50.27
4	7.228	3.594	73.327	137.62	2.462	17.422	23.76	>1000

CORE RESISTIVITY TEST SYSTEM

A core resistivity system known as an Electrocapillarometer (CAPRI) was used to perform tests at elevated confining pressure and temperature conditions. A sample at a time is inserted in an electrode sleeve for measurement. The electrode sleeve contains two embedded ring electrodes, 3.81 cm apart, centered along the plug sample to read the four-pole conductivity. In fact, the system reads the core conductivity between the end caps, the upper conductivity for the core portion between the upper embedded electrode and the base cap, and the lower conductivity between the lower embedded electrode and the base cap. Well calibrated core conductivity readings between the end caps were used in calculations, whereas poor calibrated upper and lower readings were used to observe the conductivity trend. During the multi salinity tests, the core, upper, and lower conductivities were monitored while different salinity brines were flooded through the core plugs.

EXPERIMENTAL PROCEDURES AND TEST CONDITIONS

Prior to the electrical tests, the plug samples were cleaned in a Soxhlet by circulating toluene and alcohol, then they were dried at a low temperature in a humidity-controlled oven in order to prevent dehydration of the clay minerals. The oven temperature was set at 60 ^{o}C and humidity at 45 percent while drying [7,8]. Basic core properties of plugs, such as porosity, gas permeability, and grain density were determined under 2,000 psi confining pressure prior to the electrical testing.

Multiple salinity electrical tests were conducted by mounting a sample in the hydraulic cell, applying 2,000 psi confining pressure and 65°C. Following the stabilization of the confining pressure and temperature, circulation of the 250 kppm brine was started and continued until the core conductance was stabilized. Circulation at each salinity step lasted until at least 15 pore volumes of brine had circulated through the sample. The resistivity of the effluent brine was monitored to make sure that the previous brine was completely displaced from the core. The circulation time for each brine step took three to six hours in permeable samples and two to three days in some low permeability samples.

Ten different concentrations of NaCl brines were used in the experiments. Each test was started with the highest salinity brine and sequentially continued with lower salinities. Electrical conductances at three different intervals of core plugs were monitored continuously. Figure 4 shows a typical conductance versus elapsed time plot of the test for Sample 395. Conductances decreased as salinity decreased. In highly permeable samples conductivity dropped rapidly when less salty brine was used, but later slightly increased as temperature stabilized.

DISCUSSION OF RESULTS

Test Results

The core conductance readings at the equilibrium states of different salinities were used in interpreting the effect of clay on rock conductivity. Conductivity data of tested samples is

shown in Table 2. The Co - Cw plots for all the samples in Figure 5 show linear alignments at high salinity points and faster decreasing Co values for brines with Cw's lower than 6 mho/m (19.8 kppm). The sharp decrease in conductivity with decreasing concentration of electrolyte in the dilute range of the Co versus Cw curve, as observed in the experiment, is attributed to a decreasing exchange-cation mobility [4]. Above the relatively high concentration of equilibrating electrolyte solution, the rock's conductivity increases linearly with increasing solution conductivity because the exchange-cation mobility reaches its maximum value and remains constant [9].

Table 2. Mutiple-salinity electrical measurement data.

Brine		**Samples**								
Salinity (kppm)	**Cw (mho/m)**	**393 (mho/m)**	**395 (mho/m)**	**1/1 (mho/m)**	**1/2 (mho/m)**	**1/3 (mho/m)**	**1/6 (mho/m)**	**1/7 (mho/m)**	**1 (mho/m)**	**4 (mho/m)**
250	**44.348**	1.650	1.910	1.547	0.850	2.135	0.946	0.999	1.7500	5.009
150	**33.618**	1.259	1.468	1.200	0.681	1.700	0.857	0.820	1.3662	3.990
100	**24.814**	0.957	1.122	0.940	0.534	1.314	0.623	0.641	1.0899	2.822
50	**13.447**	0.548	0.663	0.557	0.313	0.766	0.381	0.405	0.6370	1.667
25	**7.444**	0.343	0.392	0.325	0.204	0.429	0.233	0.233	0.3962	0.898
15	**4.632**	0.251	0.253	0.219	0.142	0.280	0.151	0.126	0.2708	0.537
8	**2.573**	0.169	0.158	0.138	0.095	0.169	-	0.078	0.1608	0.312
4	**1.279**	0.097	0.085	0.087	0.065	0.101	-	0.050	0.1024	0.185
2	**0.664**	0.053	0.067	0.057	0.044	0.061	-	0.037	0.0638	0.099
1	**0.345**	0.028	0.037	0.038	0.033	0.039	-	0.025	0.0463	0.056

The relationships obtained from the linear regression analyses of high salinity points were used to determine the formation factor (F^*) of the shaly sand and the values of the shaliness term (BQv). All calculated and interpreted final results are shown in Table 3. The formation factors (F^*) of the shaly sand is calculated as the reciprocal of the slope of the linearly fitted C_o-C_w curve, and the shaliness term (BQv) is equal to the value of Cw when Co is zero. The regression analyses of the nine samples have been averaged, and the following Co versus Cw relationship has been produced to represent the tested Jouf sandstone facies:

$$Co = 0.0319\ Cw + 0.0826 \qquad (2)$$

The F^* values for the Jouf samples varied between 9.091 and 53.763, and these values revealed an average F^* of 31.305 for the reservoir rock. The values of the shaliness term (BQv) showed a rather uniform distribution, where the minimum and maximum values were 0.0160 and 0.0340 mho/cm, respectively. A representative BQv was calculated to be 0.0258 mho/cm for the tested sandstone samples.

B is introduced as the equivalent conductance of the counter ions as a function of solution conductivity. In another term, it is the factor relating the cation exchange capacity per unit pore volume (Qv) to shale conductivity. The parameter B is a function of brine resistivity (Rw) and temperature (t), and can be calculated by the following expression [11]:

$$B = (-1.28 + 0.225t - 0.0004059t^2) / (1 + Rw^{1.23} (0.045t - 0.27)) \quad (3)$$

Using this equation, B at 65°C temperature is calculated to be 0.113 mho cm^2 / meq for 250 kppm brine concentration, where Rw=0.023 ohmm. Knowing B, the cation exchange capacity per unit pore volume can be calculated. The average cation exchange capacity per unit pore volume for the tested Jauf samples is determined to be 0.228 meq/cc.

Table 3. Summary of the results obtained from the multi salinity conductivity tests.

Parameter	Sample 393	Sample 395	Sample 1	Sample 4	Sample 1/1	Sample 1/2	Sample 1/3	Sample 1/6	Sample 1/7	Average
Co vs Cw curve fit	Co = 0.0354Cw + 0.0759	Co = 0.0408Cw + 0.1013	Co = 0.0388Cw + 0.0933	Co = 0.1100Cw + 0.1755	Co = 0.0333Cw + 0.0868	Co = 0.0186Cw + 0.0622	Co = 0.0461Cw + 0.1287	Co = 0.0235Cw + 0.0585	Co = 0.0217Cw + 0.0738	Co = 0.0319Cw + 0.0826
F^* = (1/ Slope)	28.249	24.510	25.773	9.091	30.030	53.763	21.692	42.553	46.083	31.305
BQv (mho/cm)	0.0214	0.0248	0.0240	0.0160	0.0261	0.0334	0.0279	0.0249	0.0340	0.0258
Qv for 250 kppm brine (meq/cc) (Qv = BQv/0.113)	0.189	0.219	0.212	0.141	0.230	0.295	0.246	0.219	0.300	0.228
Shale effect for 250 kppm brine (BQv / Cw)	0.05	0.06	0.05	0.04	0.06	0.08	0.06	0.06	0.08	0.06
Hoyer and Spann critical salinity (Cwc=BQv/0.1)	Cwc=21.44 mho/m (76 kppm)	Cwc=24.83 mho/m (92 kppm)	Cwc=24.05 mho/m (90 kppm)	Cwc=15.95 mho/m (55 kppm)	Cwc=26.07 mho/m 100 kppm)	Cwc=33.44 mho/m (140 kppm)	Cwc=27.92 mho/m (105 kppm)	Cwc=24.89 mho/m (92 kppm)	Cwc=34.01 mho/m (150 kppm)	Cwc=25.84 mho/m (100 kppm)

Shaliness Effect

The effect of shaliness on electrical conductivity in a rock can be quantified using the following equation:

$$F^* / F = (1 + BQv / Cw) \quad (4)$$

where: F = Cw / Co, Archie's definition of the formation factor.

Using Hoyer and Spann [10], the significance of the clay effect was evaluated. According to their work, if the term BQ_v/C_w is less than 0.1, then the shaliness effect will be less than 10 percent. In this case, the shaliness effect can be neglected for that concentration and the clean sand relationships can be used safely. When the shaliness effect is more than 10 percent, it should be accounted for in the interpretations. The shaliness effects calculated for the Jouf samples at a 250 kppm concentration varied between 4 and 8 percent. Therefore, it can be concluded that the shaliness effect is not at a significant level in the reservoir.

Figure 6 indicates the ranges of formation-water resistivity, Rw, and shale conductivity, BQv, within which the Archie equation and shaly sand algorithms of the type of Waxman and Smits [4] are likely to be valid [12]. Samples from the Jauf reservoir fall into the Archie region in this plot, but close to the boundary with shaly sand models.

Critical Salinity

Moving from the same concept, BQv / 0.1 was used to find a critical salinity for each sample. The calculated critical salinities ranged from 55 to 150 kppm, resulting in an average value of 100 kppm. Since the formation brine and mud filtrate are much higher than this range, using the conventional clean sand relationships is safe for the Jauf reservoir. If the reservoir is treated with a mud filtrate or any other brine whose concentration is lower than 100 kppm, shaliness correction is required.

Salinity Dependence of the Formation Factor

The Archie [1] formation factor (F) is calculated as the ratio of the conductivity of brine (Cw) to the conductivity of fully brine saturated rock (Co) and it is independent of the salinity of the brine in clean sandstones. However, in shaly sands, it decreases as salinity decreases, as a result of the contribution of the clay to conductivity. Formation factor changes with salinity are shown in Figure 7. The decrease of F with decreasing Cw reveals a log-linear relationship. The slope of this log-linear trendline depends on the shaliness effect. A plot of shaliness effect (BQv) versus slope for tested samples is given in Figure 8.

CONCLUSIONS

The Jauf Formation consists of sandstone and shale. Semi-consolidated sandstone interlayers form the reservoir pockets. These reservoir intervals contain authigenic clay either lining or filling the pore spaces. Clay is mostly illite, some chlorite and rarely mixed layers of smectite/illite. Clay minerals lower resistivity and cause high irreducible water saturation.

Experiments showed that the effect of clay conductivity (BQv/Cw) in the Jauf reservoir at reservoir salinity is around 6 percent. This insignificant effect is due to illite and chlorite type clays, which have a low-to-moderate cation exchange capacity, and the high salinity in the reservoir. Therefore, the Archie equation can be used for interpreting water saturation in the Jauf reservoir. The calculations indicated a critical salinity of 100 kppm for 10 percent clay effect on the conductivity of the reservoir rock.

The formation factor F, calculated as the ratio of Cw to Co, is not constant for the Jauf samples due to clay content. It decreases as the brine concentration decreases. The slopes of fitted logarithmic curves increases as the shaliness effect increases (BQv). This relationship can be used in determining a preliminary estimate of shale effect if the slope is determined correctly from only two brine tests.

ACKNOWLEDGEMENT

The authors acknowledge the supports of managements of the Research Institute of King Fahd University of Petroleum and Minerals, and Saudi Aramco for this study under KFUPM/RI Project No. 21170. Acknowledgements are also extended to SCA reviewers Olga Vizika and Paul Worthington, who suggested improvements.

NOMENCLATURE

C_o: Conductivity of rock fully saturated with brine solution (mho/m)
C_w: Conductivity of the brine (mho/m)
F: Formation resistivity factor
F^*: Formation factor for shaly sandstone
Q_v: Cation exchange capacity per unit pore volume (meq/cc)
B: Equivalent conductance of clay exchange cations at room temperature (mho cm^2/meq)
BQv: Shaliness effect on conductivity (mho/cm)

REFERENCES

1. Archie, G. E., The electrical resistivity log as an aid in determining some reservoir characteristics. *Transactions, AIME,* (1942) vol. 31, p. 350-366.
2. Jing, X.D. and Archer, J. S., An improved Waxman-Smits model for interpreting shaly sand conductivity at reservoir conditions. (1991) *Trans SPWLA 32nd Annual Logging Symposium, Midland, Texas*, 16-19 June.
3. Jing, X. D., Electrical properties of shaly rocks at reservoir conditions. *PSTI Technical Bulletin,* (1992) no.1.
4. Waxman, M. H. and Smits, L. J. M., Electrical conductivities in oil-bearing shaly sands. SPE 42nd Annual Meeting, Houston, Texas, 1967. *Soc. of Petroleum Engineers Journal*, (1967) vol. 8, p. 107-122 (1968).
5. Yuan, H. H., Salinity dependence of the shaly sand formations. (1991) *SPE22665, 66th Annual Technical Conference and Exhibition of the SPE*, Dallas, TX, October 6-9.
6. Folk, R. L. *Petrology of Sedimentary Rocks*. Austin, Texas, Hemphill's Book Store, (1968), p. 170.
7. Soeder, D. J., Laboratory drying procedures and the permeability of tight sandstone core. *SPE Formation Evaluation*, (1986) vol.1, no.1, p.16-22.
8. Soeder, D. J. and Doherty, W. G., The effects of laboratory drying techniques on the permeability of tight sandstone core. (1983) *SPE/DOE Low Permeability Gas Reservoir Symposium,* Paper SPE 11622, Denver
9. Waxman, M. H. and Thomas, E. C., Electrical conductivities in shaly sands, I. The relation between hydrocarbon saturation and resistivity index, II. The temperature coefficient of electrical conductivity. *JPT*, (1974) vol. 26, p. 213-225.
10. Hoyer W. A. and Spann, M. M., Comments on obtaining accurate electrical properties of cores. (1975) *SPWLA 16th Annual Logging Symposium*, 4-7 June.

11. Juhasz, I., Normalized Qv – the key to shaly sand evaluation using the Waxman-Smits equation in the absence of core data. (1981) *Transactions SPWLA 22nd Annual Logging Symposium*, Z1-36.
12. Worthington, P. F., Recognition and evaluation of low resistivity pay. *Petroleum Geoscience*, (2000) vol. 6, p. 77-92.

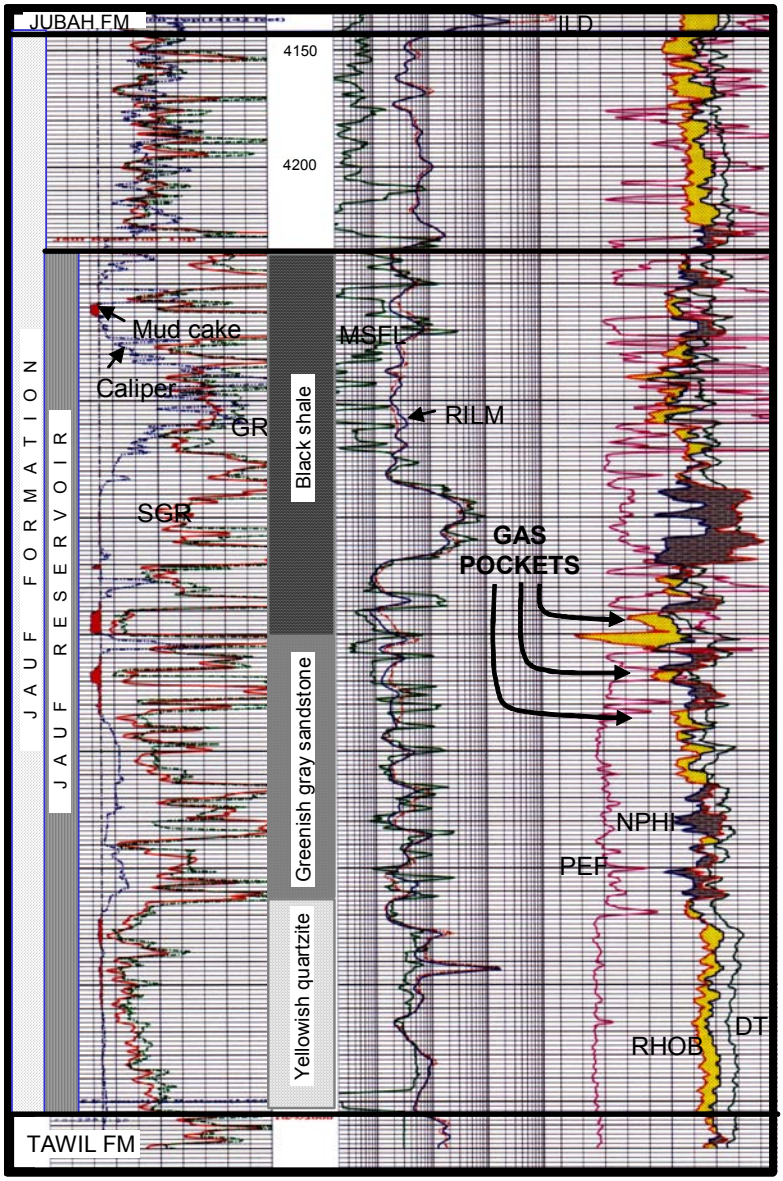

Figure 1. Open hole well logs of the Jauf reservoir showing major lithofacies zones and gas occurrences.

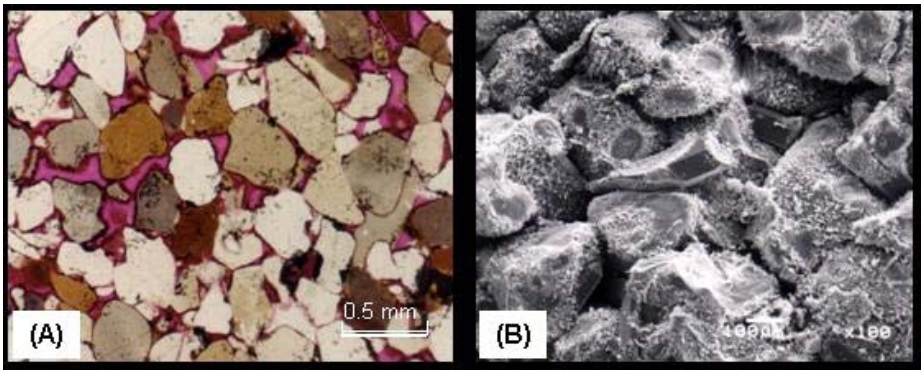

Figure 2. (A) thin section photomicrograph showing rounded terrigenic quartz grains and euhedral or pore filling authigenic quartz. Dark rims around pore spaces are pore lining clay (plain polarized light). (B) Low magnification SEM view showing clay-coated terrigenic quartz grains and euhedral hexagonal quartz crystal developments. The bold spots on the grains are contact points of removed grains. Note the absence of clay on authigenic quartz crystals.

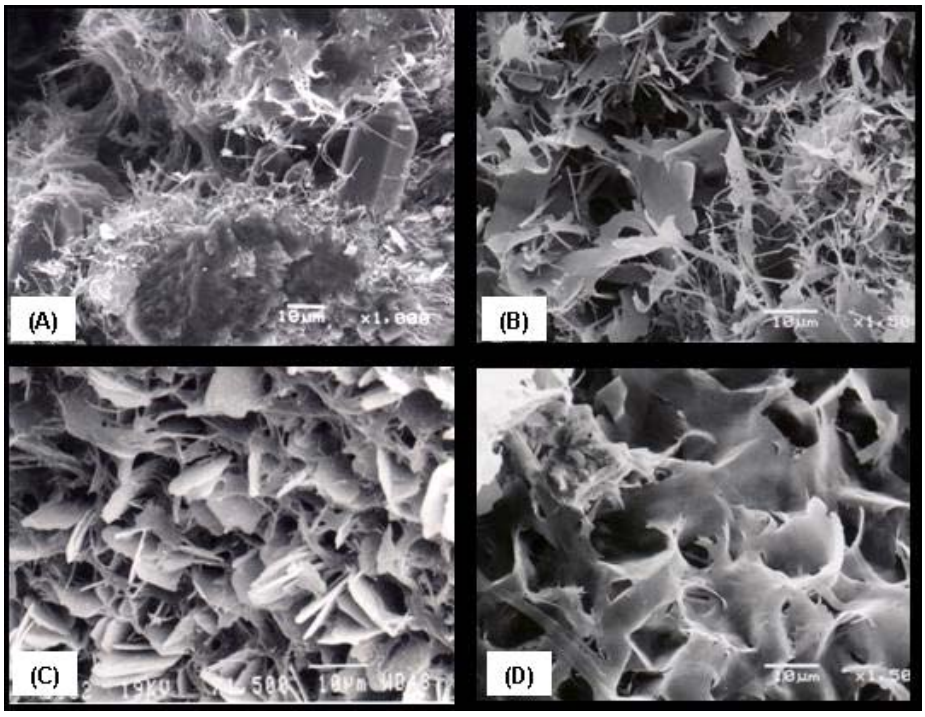

Figure 3. SEM photomicrographs of various authigenic clay morphologies observed in the Jauf Sandstone samples: (A) illite coating quartz grains then becoming filamentous and bridging the pore, (B) flaky and ribbon illite, (C) pore lining chlorite rosette crystals and some fibreous illite, (D) honeycomb mixed layer illite/smectite.

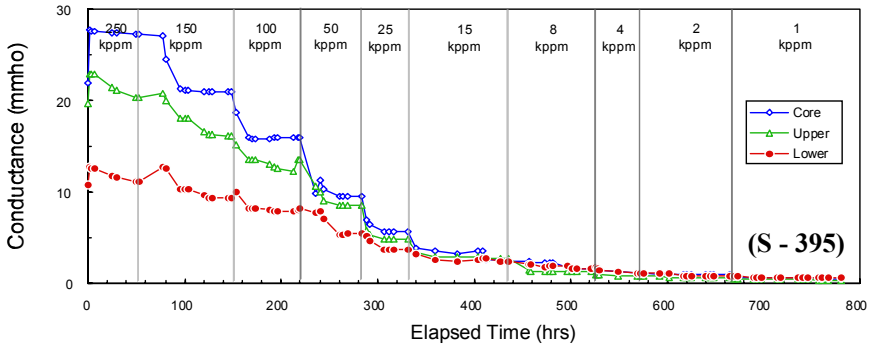

Figure 4. A typical conductance versus elapsed time plot for multi-salinity test of Sample 395.

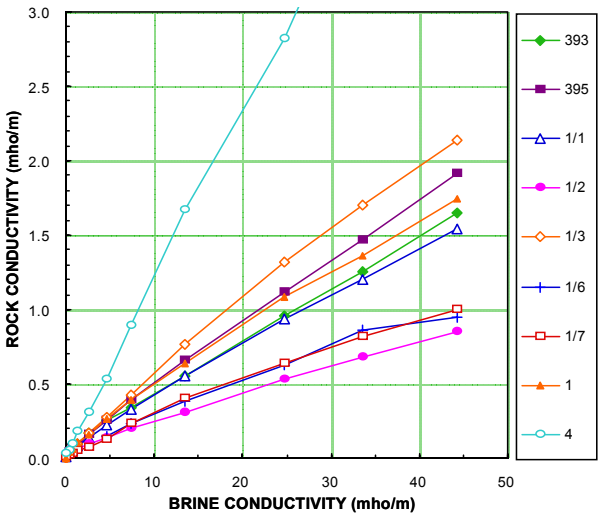

Figure 5. Rock conductivity versus brine conductivity plots.

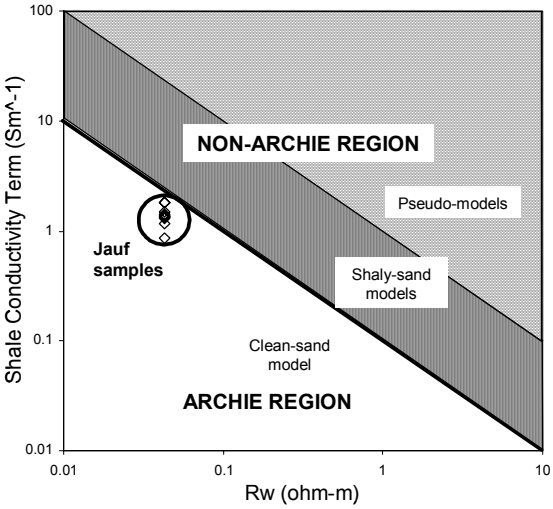

Figure 6. Applicability of the water saturation equations in the Jauf reservoir (after Worthington, 2000).

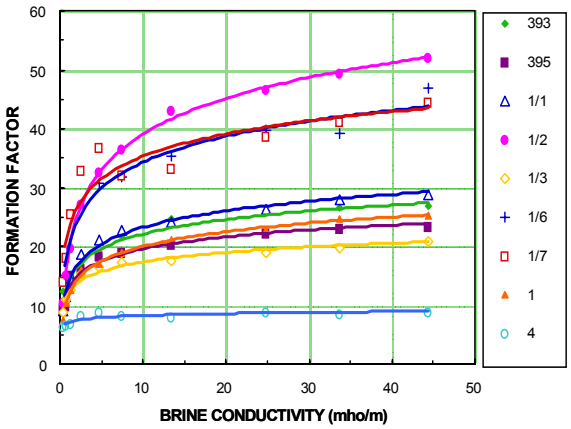

Figure 7. Formation factor variations with brine salinity.

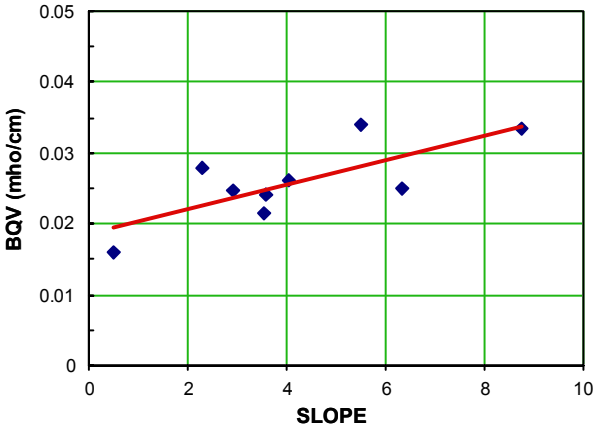

Figure 8. Dependence of the shaliness effect (BQv) on the logarithmic trendline slopes of the formation factor curves in Figure 7.